Environmental Science & Technology

pubs.acs.org/est

Article

Macromolecular Characterization of Compound Selectivity for Oxidation and Oxidative Alterations of Dissolved Organic Matter by Manganese Oxide

Jianchao Zhang, Amy M. McKenna, and Mengqiang Zhu*

Cite This: *Environ. Sci. Technol.* 2021, 55, 7741−7751

Read Online

ACCESS | Metrics & More | Article Recommendations | Supporting Information

ABSTRACT: Manganese (Mn) oxides can oxidize dissolved organic matter (DOM) and alter its chemical properties and microbial degradability, but the compound selectivity for oxidation and oxidative alterations remain to be determined. We applied ultrahigh mass spectrometry to catalog the macromolecular composition of Suwannee River fulvic acid (SRFA) before and after oxidation by a Mn oxide (δ-MnO_2) at pH 4 or 6. Polycyclic aromatic hydrocarbons, polyphenols, and carbohydrates were more reactive in reducing δ-MnO_2 than highly unsaturated and phenolic (HuPh) compounds and aliphatics, but highly abundant HuPh contributed the most (~50%) to the overall reduction of δ-MnO_2. On average, oxidized species had higher molecular weights, aromaticity, carbon unsaturation degree, nominal oxidation state of carbon, and oxygen and nitrogen contents but were lower in hydrogen content compared to unoxidized species. The oxidation decreased these molecular indices and oxygen and nitrogen contents but increased the hydrogen content, with stronger changes at the lower pH. This DOM oxidation on polar mineral surfaces was more selective but shared similar selectivity rules to adsorption. The abiotic oxidation resembles microbial oxidative degradation of organic matter, and Mn oxide−oxidizable carbon may be a useful index for detection and identification of labile organic carbon.

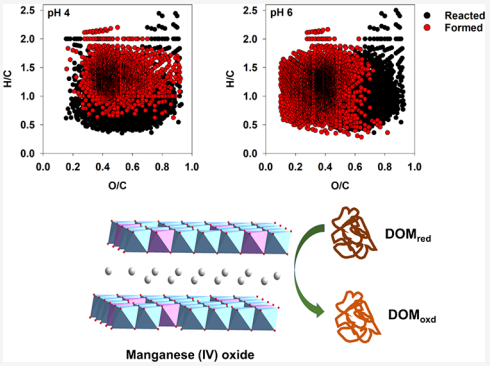

KEYWORDS: *dissolved organic matter, manganese oxide, ultrahigh resolution mass spectrometry*

INTRODUCTION

Dissolved organic matter (DOM) is an important organic carbon (C) pool in ecosystems and plays multiple roles in the environment. For example, interactions with DOM affect fate, transport, bioavailability, and toxicity of metals and nanoparticles in the environment.[1−3] DOM actively participates in C cycling through promoting the formation of stabilized mineral-associated organic matter (OM).[4,5] Although microbial oxidation is the major DOM degradation pathway, DOM can also be degraded through abiotic oxidation by environmental oxidants (e.g., radicals,[6] H_2O_2,[7] manganese (III,IV) oxides (referred to as Mn oxides hereafter),[8−14] and Mn(III)-ligand complexes[15,16]) and industrial oxidants (e.g., permanganate, chlorine, and ozone in water treatment).[17,18] Oxidation can substantially alter DOM composition and thus chemical properties and microbial degradability.[17,18]

Manganese oxides are ubiquitous oxidants in both natural and engineered environmental systems.[19,20] Chemical oxidation of DOM by Mn oxides can occur in the photic zone of aquatic systems,[21] soils,[22] lacustrine and pelagic sediments,[23,24] and Karst caves[25] under oxic and suboxic conditions, although microbial dissimilatory reduction of Mn oxides dominates under anoxic conditions.[26] Mn oxides in some of these environments are not as abundant as other minerals. However, the oxidation of DOM by Mn oxides can be disproportionally important as Mn(II)-oxidizing microorganisms are widespread and can recycle the reduction product Mn(II) to Mn oxides using O_2 as an oxidant,[27] rendering Mn oxides as catalysts because ultimately DOM is oxidized by O_2 in the system. Similar to Mn(II)-oxidizing microorganisms, mineral surfaces can also catalyze the oxidation of Mn(II) by O_2 and couple the Mn redox cycle with oxidation of OM.[28]

Dissolved OM is composed of thousands of ill-defined macromolecular compounds that vary in elemental composition, molecular structure, and chemical properties. They can be classified into aliphatic hydrocarbon and carbohydrates as well as aromatic compounds that include polycyclic aromatic hydrocarbon (PAH), polyphenols, and phenols.[29] Upon reacting with Mn oxides, the compounds can adsorb on the oxide surfaces, some of which subsequently donate electrons to

Received: February 24, 2021
Revised: April 23, 2021
Accepted: April 23, 2021
Published: May 11, 2021

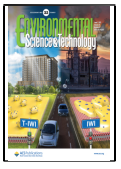

https://doi.org/10.1021/acs.est.1c01283
Environ. Sci. Technol. 2021, 55, 7741−7751

the oxides and get oxidized. The oxidation produces modified macromolecular compounds and low-molecular-weight organic acids (e.g., pyruvate and acetate) with minor gases (e.g., CO_2 and CO).[8,9,11,12,28] The ability of DOM compounds to adsorb on Mn oxide surfaces and the potentials to act as reductants in the resulting charge complexes affect the oxidation of the compounds by the oxides. Aromatics and compounds of high molecular weights (MWs) were found to preferentially adsorb on iron (III) oxide surfaces, resulting in molecular fractionation.[29,30] Such selective adsorption was suggested to occur in Mn oxide−DOM systems as well.[13] Aromatics (mainly phenols) were also found to be more reactive than others in reducing Mn oxides.[31] In addition, the increasing concentration of reduction product Mn(II) and other structural and compositional changes of Mn oxides induced by DOM reduction can substantially enhance DOM adsorption[13] and may affect the adsorption and oxidation selectivity.

Several outstanding questions about the Mn oxide−DOM system remain to be answered. Not all compounds in DOM can be oxidized by Mn oxides, but the proportion of the oxidizable compounds has not been quantified. In addition, what other molecular characteristics besides aromaticity differentiate the oxidizable from nonoxidizable ones, i.e., the compound selectivity rule for oxidation remains to be determined. At last, the oxidative changes are unclear at the macromolecular level, although the low-molecular-weight products have mostly been identified.[8,9,11,12,28] The present study, therefore, is aimed at quantifying the degree of oxidation, determining the compound selectivity for oxidation, and characterizing the oxidative alterations by Mn oxides for DOM as a single pool or for each compound class at the macromolecular level using electrospray ionization (ESI) ultrahigh-resolution Fourier transform ion cyclotron resonance mass spectrometry (FT-ICR MS). δ-MnO_2, a common layered Mn oxide and an analogue to naturally occurring Mn oxides, and Suwannee River fulvic acid (SRFA) were used as model reactants to provide a proof of concept, while both Mn oxides and DOM are highly heterogeneous in the environment.[32,33] To address those questions, we compared the macromolecular signature before and after the reaction of SFRA with δ-MnO_2 to identify the compounds that were reacted, formed (i.e., newly produced), and persistent.

EXPERIMENTAL SECTION

δ-MnO_2 was synthesized with $MnCl_2$ to reduce $KMnO_4$ (Supporting Information, Text S1). Suwannee River fulvic acid was purchased from the International Humic Substance Society.

DOM Oxidation by δ-MnO_2. Batch oxidation experiments were conducted by reacting SRFA with δ-MnO_2 at pH 4 or 6 for 600 h. The total volume of the reacting suspension was 400 mL, containing 600 mg/L SRFA, 6.0 g/L δ-MnO_2, and 50 mL of NaCl in a 1 L glass bottle wrapped with aluminum foil. The ratio (0.1) of SRFA to δ-MnO_2 is relevant to the Mn-rich environment and led to a partial reduction of δ-MnO_2.[13] The suspension was constantly shaken in a thermostat shaker (25 °C), and the pH was maintained at the target pH by adding 0.1 M NaOH or HCl during the experimental period. Both the SRFA stock solution and the δ-MnO_2 suspension were pre-equilibrated at the target pH overnight prior to mixing. The experiments were performed in a triplicate.

To determine the oxidation kinetics, an aliquot (4.2 mL) of suspension was collected at predetermined time intervals and centrifuged at 8000 rpm for 5 min. The supernatant was filtered with a 0.22 μm PTFE syringe filter and stored at 4 °C prior to the measurements of DOC concentration, dissolved Mn(II) concentrations, and E_2/E_3 ratios (absorbance at 254 nm to that at 365 nm) using UV−vis spectroscopy. Details are provided in Text S2. The filtrate obtained at 504 h was used for characterizing the composition of OM that remained in the solution using FT-ICR MS.

The changes of OM composition after 504 h of oxidation by δ-MnO_2, when the reaction reached a pseudo-equilibrium, were determined by comparing the composition of the unreacted (at 0 h) and reacted SRFA in the entire suspension, with the latter comprising OM both remained in solution and adsorbed on the solid. The organic matter that remained in the solution could not accurately reflect the oxidation in the system because a large portion of OM compounds was adsorbed on the solid. The organic matter in the entire system was obtained by mixing the OM in the solution and the OM desorbed from the solid by 0.1 mM NaOH (pH 10) under anoxic conditions. While the extraction with 100 mM NaOH solution can change OM composition,[34] 0.1 mM NaOH had much lower alkalinity and was not expected to affect OM composition much. The FT-ICR MS analysis did show only a subtle difference in composition between 0.1 mM NaOH-treated SRFA solution and untreated one (Text S3, Table S1, and Figure S2). The recovery rate of OM for the above extraction was estimated to be 90.4%. Details for preparing the reacted SRFA sample, including the OM of the entire system, are provided in Text S3.

ESI FT-ICR MS Characterization. Electrospray ionization (ESI) in negative ion mode, coupled to FT-ICR MS, has been increasingly used to characterize DOM composition from nearly every type of aqueous, soil, and sedimentary OM sources.[32,35−38] Aqueous samples were isolated by solid-phase extraction (SPE)[39] prior to the negative-ion ESI 21-T FT-ICR MS measurement.[40−43] Each mass spectrum was converted to Kendrick mass, internally calibrated, and elemental compositions assigned with PetroOrg.[44−46] Only formulae present in all triplicates were selected for the following data analyses, and the disregarded formulae accounted for 9−14% of the total. Formulae introduced by contamination were negligible. Various molecular indices were calculated from the formulae, including modified aromaticity index (AI_{mod}),[47] double bond equivalence (DBE), and nominal oxidation state of carbon (NOSC).[48,49] Detected DOM compounds were categorized into the following five compound classes based on neutral elemental compositions,[29] (1) polycyclic aromatic hydrocarbons (PAHs; $AI_{mod} > 0.66$), (2) polyphenols ($0.66 \geq AI_{mod} > 0.50$), (3) highly unsaturated C and phenolic formulas (HuPh; $AI_{mod} \leq 0.50$ and $H/C < 1.5$), (4) aliphatic compounds ($1.5 \leq H/C < 2$), and (5) carbohydrate compounds ($H/C \geq 2$), based on relative-abundance-weighted averages for compounds within each mass spectrum. Compounds were further grouped based on molecular weight: high (450−∼900 Da), middle (300−450 Da), and low (150−300 Da).[50] Details on SPE, instrumentation, data collection, and formulae assignments are provided in Texts S4 and S5.

To determine the changes in OM composition after the reaction with δ-MnO_2, we grouped the organic compounds in the reacted SRFA into the following three pools: (1) selectively oxidized or called reacted compounds (OM_{rctd}), (2) newly produced or called formed compounds (OM_{frmd}), and (3) persistent compounds (OM_{pers}). OM_{rctd} contained the compounds present in the unreacted SRFA but absent in the reacted

https://doi.org/10.1021/acs.est.1c01283
Environ. Sci. Technol. 2021, 55, 7741−7751

SRFA; the compounds in OM_{frmd} were present in the reacted SRFA but not in the unreacted FA. The compounds in OM_{pers} can be found in both the reacted and unreacted SRFA. By doing this, we assumed that if a compound was oxidizable, nearly all molecules of this compound must be oxidized and that none of the compounds in OM_{pers} was oxidized. The assumptions were reasonable considering that after 504 h, the net oxidation was negligible because dissolved Mn(II) concentration did not increase with time anymore (Figure 1). It was also assumed that the oxidation did not produce compounds having the same molecular formulae as any in OM_{pers}. The above assumptions did not consider the existence of isomers in SRFA that differ in reactivity and thus may appear in both OM_{rctd} and OM_{pers}. Ion suppression during FT-ICR MS data collection was not considered either, which could result in misidentification of suppressed compounds as ones to be oxidized. Despite these potential issues, the assumptions allowed us to have approximate catalogs of the compounds that were reacted, persistent, and formed and thus to gain deep insights into the reaction system. Similarly, each class of compounds (i.e., PAH, carbohydrates, etc.) was grouped into reacted, persistent, and formed pools as well, allowing for detailed analyses of how δ-MnO_2 oxidized and altered each compound class. Note that the formed compounds in each class could be produced from any compound class. Thus, a comparison between the reacted and formed compounds in a class simply indicates overall what new compounds were formed to replace the old ones (i.e., the selectively oxidized) upon the oxidation of all classes, rather than how the oxidation altered the compounds originally present in that class.

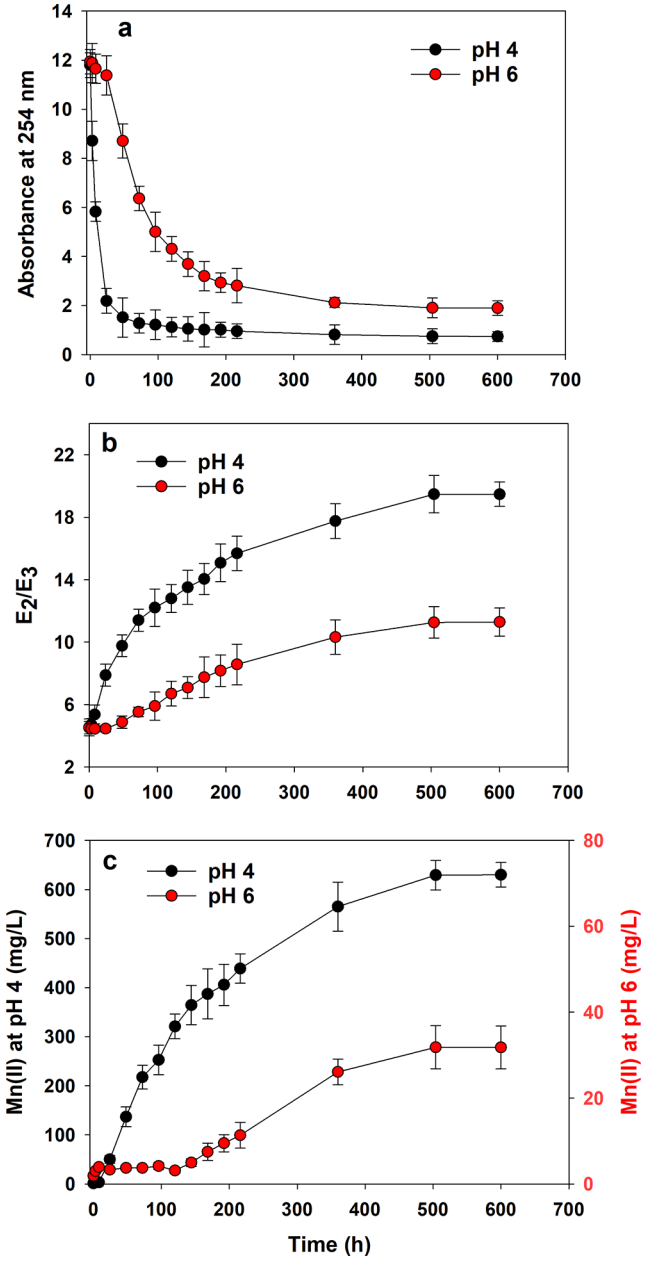

Figure 1. Ultraviolet absorbance at 254 nm (a), E_2/E_3 ratios (b), and Mn(II) concentrations (c) in the solution phase during the reaction of SRFA with δ-MnO_2 at pH 4 and pH 6. The reported UV−vis absorbance values in (a) were the measured values multiplied by the dilution times. Details provided in Text S2.

RESULTS AND DISCUSSION

Adsorption and Oxidation of DOM by δ-MnO_2. The reaction reached a pseudo-equilibrium at 504 h because the concentration of dissolved organic matter and Mn(II) and E_2/E_3 ratios of the solutions did not change afterward (Figure 1). At 504 h, 93 and 83% of OM were removed from the solution at pH 4 and 6, respectively (Figure 1). The OM removal was faster than the production of dissolved Mn(II) (Figure 1), indicating that the OM oxidation was slower than its adsorption.[11,13] The faster production of much more dissolved Mn(II) at pH 4 than that at pH 6 (Figure 1) is consistent with low pH favoring OM oxidation by Mn oxides due to multiple mechanisms.[31] Stronger Mn(II) adsorption on δ-MnO_2 at pH 6 than at pH 4 also contributed to the lower dissolved Mn concentration at pH 6.[13] The E_2/E_3 ratio of the solution increased with reaction time and was higher at pH 4 than at pH 6 at a given time, suggesting decreased DOM aromaticity, MW, and probably electron-donating capacity[51,52] with larger decreases at lower pH. The E_2/E_3 ratios were surprisingly high toward the end of the reaction (Figure 1), which was also observed previously[13] and can be ascribed to oxidative alterations of DOM.[53]

The composition of macromolecular compounds in the entire system differed from that present only in the solution at 504 h. Since the oxidation essentially stopped at 504 h, the difference between the two can be ascribed to adsorption-induced molecular fractionation. The number of different organic compounds in the solution (12650 at pH 4 or 14441 at pH 6) was lower than that in the entire system (13407 at pH 4 or 15458 at pH 6), so did for each compound class (Table 1), indicating complete removal of some compounds from the solution by adsorption on δ-MnO_2. The adsorption preferentially removed aromatics and enriched aliphatic and carbohydrate compounds in the solution at both pH (Table 1), similar to DOM fractionation by Fe(III) oxides.[29,30] However, the degrees of fractionation in the present study were much lower compared to those by Fe(III) oxides.[29,30] The proportion of each compound class differed only slightly between OM in the entire system and in the solution (i.e., by 0.11−0.72% at pH 4 and 0.02−2.06% at pH 6), so did the molecular indices (Table 1). The Mn(II)-promoted DOM adsorption on δ-MnO_2 through cation bridging, and the coagulation effect was probably responsible for the weak fractionation, similar to the effects of Ca^{2+} on DOM fractionation by ferrihydrite.[54] In addition, more negative surfaces of δ-MnO_2 than Fe(III) oxides at pH 4 and 6 may contribute to the weak fractionation as well. The following discussion will be focused on the OM in the entire system.

https://doi.org/10.1021/acs.est.1c01283
Environ. Sci. Technol. 2021, 55, 7741−7751

Table 1. Molecular Characterization of the Initial SRFA (OM_0) and SRFA after 504 h of Reaction in the Entire System (OM_{tot}) and in the Solution (OM_{sol}) at pH 4 and pH 6[a]

	OM_0	OM_{tot},pH 4	OM_{sol}, pH 4	OM_{tot}, pH 6	OM_{sol}, pH 6
PAH (%)	2.56 (1211)	3.08 (932)	2.97 (882)	2.40 (1042)	3.23 (964)
Polyph (%)	10.25 (2047)	5.52 (1163)	4.80 (1085)	7.33 (1986)	7.31 (1765)
HuPh (%)	82.77 (9504)	85.69 (9602)	85.29 (9063)	84.99 (10958)	82.93 (10253)
Aliph (%)	3.71 (1105)	5.35 (1544)	5.98 (1476)	4.92 (1404)	5.50 (1401)
Carbo (%)	0.71 (129)	0.36 (166)	0.96 (144)	0.37 (68)	1.03 (58)
number of molecules	13996	13407	12650	15458	14441
high MS (%)	52.33	45.61	39.13	51.31	43.46
mid MS (%)	39.76	38.46	44.74	38.95	43.43
low MS (%)	7.91	15.93	16.13	9.74	13.11
average MS	479.46	457.46	437.57	483.98	458.62
AI_{mod}	0.33	0.29	0.29	0.31	0.30
O/C	0.52	0.52	0.53	0.46	0.49
H/C	1.13	1.19	1.22	1.18	1.20
DBE	11.04	9.79	9.12	10.78	10.02
NOSC	−0.06	−0.13	−0.12	−0.24	−0.18
C/N	66.22	46.11	49.33	100.42	57.95
C/S	361.61	186.14	200.71	299.38	281.28
CHO (%)	92.46	90.37	87.50	91.92	88.88
CHON (%)	5.79	6.43	8.95	5.18	8.07
CHOS (%)	1.38	3.21	3.55	2.90	3.05

[a]The percentage distributions of compound classes were abundance-weighted. In parentheses are the numbers of compounds in each compound class. High (450−1100 Da), mid (300−450 Da), and low (<300 Da) molecular mass (MS). Al_{mod}, modified aromaticity index; DBE, double bond equivalent; O/C, H/C, C/N, and C/S, average elemental ratios; molecular formulas in elemental groups (CHO, CHON, and CHOS); PAH, polycyclic aromatics; Polyph, polyphenols; HuPh, highly unsaturated and phenolic compounds; Aliph, aliphatic compounds; Carbo, carbohydrates.

Table 2. Molecular Compositions and Properties of the Reacted (Rctd), Formed (Frmd), and Persistent (Pers) Groups in the Entire Suspension at pH 4 or 6[a]

	OM_{tot}, pH 4			OM_{tot}, pH 6						
	Rctd	Frmd	Pers	Rctd	Frmd	Pers	Rctd only at pH 4	Rctd only at pH 6	Frmd only at pH 4	Frmd only at pH 6
PAH (%)	15.0 (549)	16.4 (270)	1.9 (662)	17.10 (465)	5.62 (296)	2.0 (746)	12.5 (227)	15.8 (143)	31.3 (190)	7.1 (216)
PolyPh (%)	32.0 (967)	3.6 (83)	9.0 (1080)	17.0 (498)	8.6 (437)	10.0 (1549)	39.7 (501)	3.9 (32)	4.3 (33)	13.2 (387)
HuPh (%)	44.6 (1498)	56.1 (1596)	84.9 (8006)	56.8 (1432)	72.8 (2886)	83.8 (8072)	46.2 (598)	65.2 (532)	39.9 (565)	72.5 (1855)
Aliph (%)	2.5 (117)	19.2 (556)	3.8 (988)	5.9 (201)	10.6 (500)	3.6 (904)	1.1 (35)	9.6 (119)	18.6 (272)	7.2 (216)
Carbo (%)	5.95 (46)	4.71 (83)	0.42 (83)	3.21 (92)	2.66 (31)	0.61 (37)	0.6 (9)	5.5 (48)	6.0 (52)	0 (0)
molec. number	3177	2588	10819	2688	4150	11308	1363	874	1112	2674
average MS	629	519	471	591	515	474	630	529	482.6	616.8
high MS (%)	82.0	57.3	50.7	77.9	64.4	51.3	83.0	74.1	38.8	77.5
mid MS (%)	10.9	23.6	41.4	18.1	25.4	40.6	6.3	20.9	37.7	13.8
low MS (%)	7.1	19.1	8.0	4.0	10.3	8.1	10.7	5.0	23.5	8.7
AI_{mod}	0.49	0.18	0.32	0.44	0.29	0.33	0.47	0.29	0.18	0.36
DBE	17.1	10.9	10.7	14.2	13.3	10.9	17.9	10.4	12.0	14.6
NOSC	0.40	−0.03	−0.09	0.72	−0.41	−0.09	0.06	0.65	0.30	−0.45
O/C	0.60	0.54	0.51	0.77	0.38	0.51	0.48	0.84	0.62	0.33
H/C	0.97	1.26	1.14	1.11	1.22	1.13	0.91	1.29	1.17	1.15
C/N	50.0	55.3	72.8	30.4	118.8	97.2	177.9	3.9	34.0	138.7
C/S	313	95	405	218	177	452	1422	160	112.5	371.9
CHO (%)	80.6	67.2	93.1	76.5	64.3	93.5	89.1	56.5	38.9	77.5
CHON (%)	10.3	26.7	5.5	10.4	24.0	5.2	9.5	38.6	37.7	13.8
CHOS (%)	2.1	6.1	1.3	3.5	11.7	1.3	1.5	4.9	23.5	8.7

[a]The values are abundance-weighted except for molecular numbers. In parentheses are the numbers of compounds in each compound class. The compositions and properties of the compounds that were oxidized at pH 4 but not at pH 6, or vice versa, are also listed.

https://doi.org/10.1021/acs.est.1c01283
Environ. Sci. Technol. 2021, 55, 7741−7751

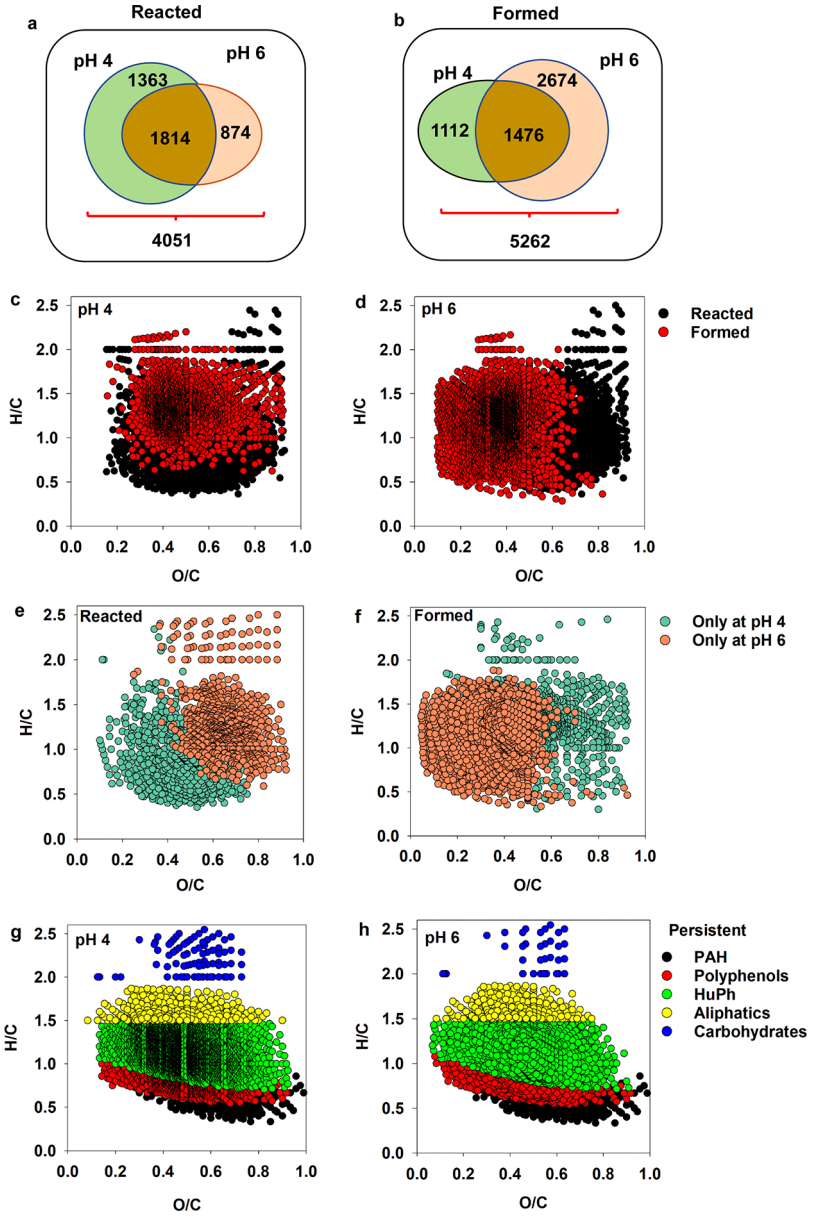

Figure 2. Numbers of the selectively oxidized (reacted) and newly formed compounds (formed) at pH 4 or 6 (a, b). The number in the overlapped region is for compounds shared at both pH levels. van Krevelen diagrams for the parent and produced compounds at pH 4 or 6 (c, d), reacted and formed compounds at pH 4 only (e) or pH 6 only (f), and persistent compounds at pH 4 (g) or 6 (h). PAH, polycyclic aromatic hydrocarbons; Polyph, polyphenols; HuPh, highly unsaturated C and phenolic compounds; Aliph, aliphatic compounds; and Carbo, carbohydrates.

The oxidation by δ-MnO_2 changed the number of compounds and molecular indices for the OM in the entire system. In total, 13 996 different compounds were detected in the unreacted SRFA, and the oxidation decreased the number to 13407 at pH 4 but increased it to 15458 at pH 6 (Table 1). At pH 4, the oxidation reduced the numbers of PAH and polyphenol compounds by 23% (1211 to 932) and 43% (2047 to 1163), respectively, but increased the number by 39.7% (1105 to 1544) for aliphatic compounds and by 28.7% (129 to 166) for carbohydrates (Table 1). A slight increase might also occur to HuPh (1%, 9504 to 9602). The increased numbers indicate that more compounds were added than removed by the oxidation to the three compound classes. Compared to that at pH 4 and pH 6, the decrease in both PAH and polyphenols and the increase in aliphatic compounds in the number of compounds were less pronounced, but the increase was much stronger for HuPh, by 15.3% from 9504 to 10958 (Table 1). In contrast to the increase at pH 4, the number of carbohydrate compounds was reduced by 47.3% at pH 6. The change in the number of compounds in each compound class translates to their relative abundance-weighted contributions, with the largest change occurring for polyphenol (decreased by 4.7% from unreacted SRFA to reacted SRFA, Table 1). As to abundance-weighted molecular indices, the oxidation increased the C/H ratio but decreased AI_{mod}, DBE, NOSC, and the O/C ratio (pH 6 only). It also decreased the proportion of high MW compounds and increased the proportion of low MW ones, and the changes were more substantial at pH 4 than at pH 6 (Table 1). Thus, on average, the oxidation broke down high-MW compounds, being more favorable at lower pH values.

Compounds Reacted. A small portion of compounds in SRFA was oxidized by δ-MnO_2 after 504 h of reaction. Only

https://doi.org/10.1021/acs.est.1c01283
Environ. Sci. Technol. 2021, 55, 7741−7751

22.7% of different OM compounds, corresponding to 12.3% abundance-weighted, were selectively oxidized at pH 4, and the proportions (10.9 and 19.2%, respectively) at pH 6 were slightly lower, calculated based on the data in Table 2. The relatively low proportions of compounds that were oxidized are consistent with the low abundance of redox-active moieties in DOM.[55] In terms of the numbers of compounds, 3177 and 2688 compounds were selectively oxidized at pH 4 and 6, respectively (Table 2), jointly 4051 different compounds, among which 1814 were oxidized at both pH, 1363 at pH 4 only, and 874 at pH 6 only (Table 2 and Figure 2a). While similar proportions of compounds were oxidized at the two pH levels, much more electrons were transferred from OM to δ-MnO_2 at pH 4 than those at pH 6, as indicated by the higher Mn(II) production (Figure 1c). Thus, the compounds oxidized at pH 4 were oxidized to higher degrees than those at pH 6. The more pronounced oxidation of SRFA by δ-MnO_2 at pH 4 could be due to changes in the protonation status of organic compounds and increased redox potential of δ-MnO_2 at lower pH.[31]

The five compound classes did not contribute equally to the overall reduction of δ-MnO_2. The contributions would be equivalent to their proportions in the reacted pool (i.e., OM_{rctd}) when assuming each oxidized molecule approximately transferred a similar number of electrons to δ-MnO_2 at a given pH. With that assumption, HuPh, Polyph, PAH, Aliph, and Carbo would contribute 44.6−55.8%, 17−32%, 15−17%, 2.5−5.9%, and 3.21−5.95% to OM_{rctd}, respectively (Figure 3b,e). The much higher contribution of HuPh than others to the reduction was likely due to its higher abundance (i.e., 83%) in unreacted SRFA (Figure 3a). The reacted pool differed greatly from the persistent pool (i.e., OM_{pers}), for which those compound classes contributed 83.8−84.9%, 9−10%, 1.9−2.0%, 3.6−3.8%, and 0.42−0.61%, respectively (Figure 3d,g). The substantial difference between the two pools indicates that the five compound classes differed in reductive activity, and some were preferentially oxidized relative to others.

The relative reactivity of a compound class may be evaluated by the proportion of the number of the reacted compounds over the total in the class, and a larger proportion suggests a higher reactivity. At pH 4, in the order of decreasing reactivity, 967 of total 2047 (47.2%), 549 of 1211 (45.3%), 46 of 129 (35.6%), 1498 of 9504 (15.8%), and 117 of 1105 (10.6%) compounds were oxidized for polyphenols, PAH, carbohydrate, HuPh, and aliphatics, respectively (Figure 3h and Table 2). The highest reductive reactivity of polyphenols is consistent with a previous report that polyphenol-like compounds in humic substances had the highest electron-donating capacity.[56] Compared to that at pH 4, the proportion of the reacted compounds at pH 6 was lower for polyphenols (498, 24.3%), PAH (465, 38.4%), and HuPh (1432, 15.1%) but higher for aliphatics (201, 18.2%) and carbohydrates (92, 71.3%) (Figure 3h and Table 2). Thus, the first three classes were more reactive at lower pH and the latter two more at higher pH. Deprotonation at higher pH can increase the reductive activity of certain organic compounds.[57,58] The surprisingly high reactivity of carbohydrate compounds at both pH 4 and 6 may be because some carbohydrate compounds had quite high O/C ratios (Figure 2e and Table S3) that favor oxidation (see discussion below). A comparison between the average molecular indices of the reacted and persistent compound pools provided further insights into the selectivity for oxidation. The abundance-weighted average indices and elemental ratios are listed in Table 2 with their number distributions plotted in Figure 4. Compared to OM_{pers},

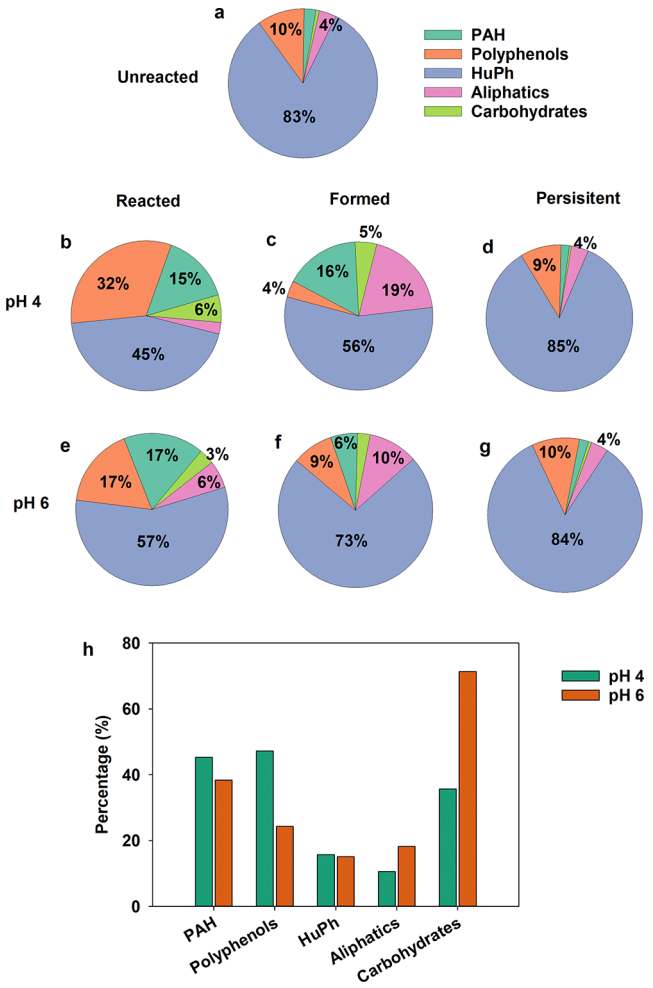

Figure 3. Abundance-weighted contributions of five compound classes to unreacted FA (a), and reacted (b, e), formed (c, f), and persistent compound pool (d, g) and percentage of the number of reacted compounds over the total number in each compound class (h). PAH, polycyclic aromatic hydrocarbons; Polyph, polyphenols; HuPh, highly unsaturated C and phenolic compounds; Aliph, aliphatic compounds; and Carbo, carbohydrates.

regardless of pH, OM_{rctd} had substantially higher average MW (629 vs 471 at pH 4 and 591 vs 474 at pH 6), AI_{mod} (0.49 vs 0.32 at pH 4 and 0.44 vs 0.33 at pH 6), NOSC (0.4 vs −0.09 at pH 4 and 0.72 vs −0.09 at pH 6), and DBE (17.1 vs 10.7 at pH 4 and 14.2 vs 10.9 at pH 6). Among them, the NOSC values differed the most, suggesting that NOSC better indicates the oxidation favorability of the compounds than other indices. On average, OM_{rctd} was also richer in O, N, and S but poorer in H compared to OM_{pers}, as suggested by the elemental ratios (Table 2). The number distributions of these molecular characteristics showed similar patterns to the averaged values, but none of these characteristics alone completely separated the compounds of the OM_{rctd} and OM_{pers} (Figure 4). A combination of two indices, such as NOSC vs DBE or the number of O in each compound, failed to separate them, either (Figure S3). Thus, the observed compound selectivity for oxidation was valid only in the sense of average molecular indices and elemental ratios and could be violated for certain compounds.

The enrichment of O and N in OM_{rctd} relative to OM_{pers} is probably because Ar-OH, R-COOH, and R-NH_2 are common redox-active moieties. That OM_{rctd} had higher AI_{mod} and DBE

https://doi.org/10.1021/acs.est.1c01283
Environ. Sci. Technol. 2021, 55, 7741−7751

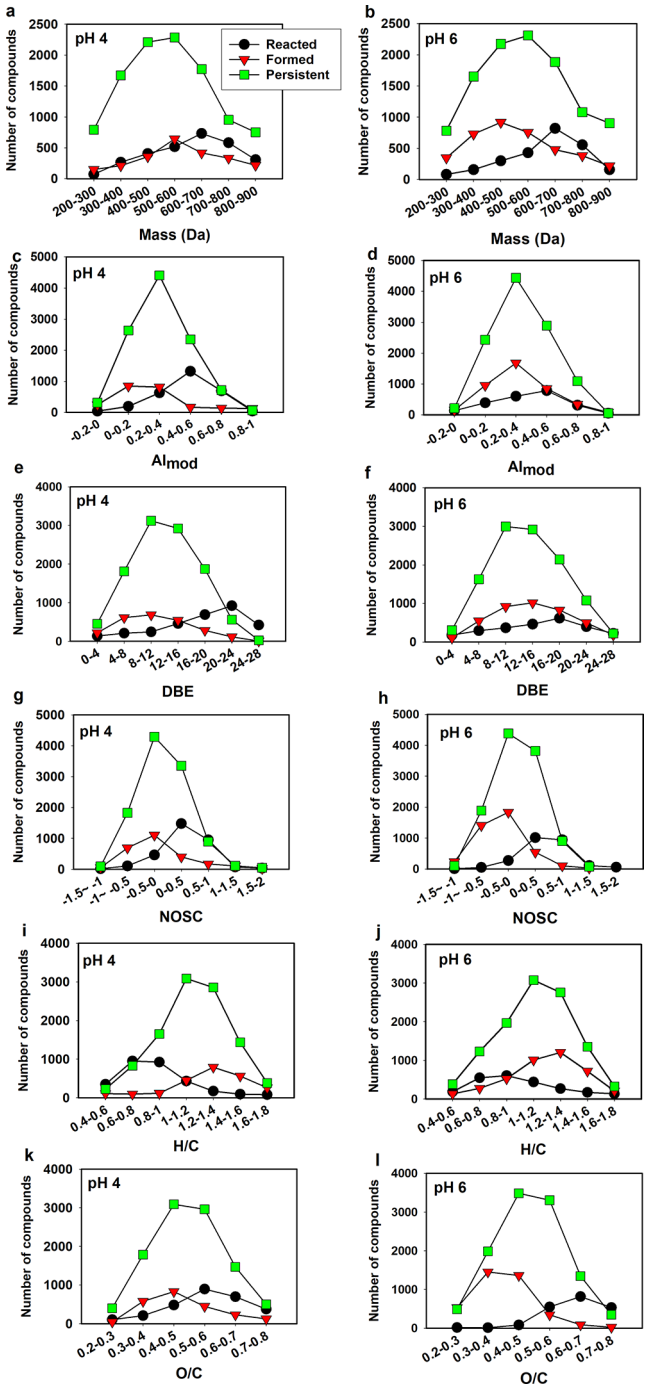

Figure 4. Number distributions of reacted, newly formed, and persistent compounds for various molecular indices at pH 4 and 6, including the modified aromaticity index (AI_{mod}), nominal oxidation state of C (NOSC), double bond equivalency (DBE), and H/C and O/C stoichiometric ratios.

than OM_{pers} is consistent with the higher reductive activity of the functional groups attached to unsaturated C than to saturated C.[59] It is unclear why OM_{rctd} had a larger AMW than OM_{pers} (Table 2), probably because OM compounds of small sizes are microbial degradation products of large ones that are relatively fresh with low decomposition degrees. Microbial degradation may have already lowered those molecular characteristics responsible for the high reactivity.[60]

The observed compound selectivity for oxidation resembles that of adsorption on reacted δ-MnO_2 (Table 1) and other metal oxide surfaces,[29,30] but the former is more selective. The similarity is not surprising because the oxidation by Mn oxides is a surface-controlled process that is determined by the accessibility of the surface to organic molecules.[31] However, the contribution of adsorption to the compound selectivity for oxidation was not that important because most OM compounds (83−93%) were adsorbed but only small portions (10.9−12.3%) of them were oxidized. That is, most adsorbed compounds had low potentials to act as reductants to reduce δ-MnO_2. The similarity in selectivity between OM adsorption and oxidation on mineral surfaces is simply because the molecular properties favoring OM oxidation also favor its adsorption, and those redox-active moieties (e.g., −OH, −COOH, and $-NH_2$) have high adsorption reactivity toward mineral surfaces. Our observations are in agreement with a recent study showing that highly redox-active DOM components were preferentially adsorbed on polar mineral surfaces (e.g., metal oxide surfaces).[61]

The potentials of OM compounds to act as reductants of δ-MnO_2 may be understood from thermodynamic perspectives. The preferential oxidation of organic compounds with higher NOSC by δ-MnO_2 complies with a thermodynamic analysis by LaRowe and Van Cappellen,[48] showing that for complete mineralization, the removal of an electron from an organic compound on average becomes thermodynamically more favorable as NOSC increases.[48] Boye et al.[60] provided empirical evidence for the applicability of the thermodynamic selectivity rule to microbial oxidative degradation of OM in natural systems. Our results suggest that the rule also applies to oxidative degradation of organic compounds via an abiotic pathway with incomplete mineralization. Again, this rule is valid for a compound pool but can be violated when analyzing a specific compound.

Compounds Formed. The newly formed compound pool (i.e., OM_{frmd}) differed greatly from the reacted pool in composition (Table 2 and Figure 4). In total, 2588 and 4150 new compounds were formed at pH 4 and 6, respectively (Table 2), and jointly 5262 new compounds, among which 1476 were at both pH, 1112 at pH 4 only, and 2674 at pH 6 only (Figure 2b). The relative abundance-weighted contributions of the five compound classes to OM_{frmd} differed from those to OM_{rctd}. PAH, polyphenols, HuPh, aliphatic, and carbohydrates, respectively, contributed 16.4, 3.6, 56.1, 19.2, and 4.71% at pH 4 and 5.62, 8.6, 72.8, 10.6, and 2.66% at pH 6 (Figure 3c,f). Compared to OM_{rctd}, the distribution of OM_{frmd} was more concentrated at HuPh and aliphatic compounds (Figure 3c,f) because the oxidation increased the numbers of compounds of the two compound classes but decreased them for the other three classes (Table 2). That is, the oxidation may form new HuPh and aliphatic compounds on the consumption of the other three, consistent with the above analysis. The remarkably increased number of compounds in HuPh after oxidation at pH 6 was likely due to the low degree of oxidation, producing new HuPh compounds that would otherwise have been further oxidized and removed from the HuPh class at pH 4.

The molecular characteristics of compounds responsible for the high selectivity for oxidation were mostly decreased to various extents. Compared to OM_{rctd}, OM_{frmd} had substantially lower AMW and AI_{mod} (0.49 vs 0.18 at pH 4 and 0.44 vs 0.29 at pH 6), indicating partial aromatic ring cleavage. OM_{frmed} also had lower DBE (11 vs 17 at pH 4 and 13.3 vs 14.2 at pH 6) and

https://doi.org/10.1021/acs.est.1c01283
Environ. Sci. Technol. 2021, 55, 7741−7751

remarkably lower NOSC (−0.03 vs 0.40 at pH 4 and −0.41 vs 0.72 at pH 6), i.e., preferential removal of highly unsaturated and oxidized C by oxidation. Permanganate oxidation was also shown to decrease aromaticity and AMW of OM.[17] Regarding elemental ratios, OM_{frmd} had lower O/C and N/C but higher H/C and S/C ratios than OM_{rctd} (Table 2), indicating that relative to C, the oxidation preferentially removed O and N but opposite for S and H. The O/N ratio of OM_{rctd} was similar to that of OM_{frmd} at pH 4 but lower (23 vs 45) at pH 6, suggesting that N and O had similar removal efficiencies at pH 4, but higher for the former at pH 6. The enrichment of S in OM after oxidation suggests that S-containing groups protect OM from abiotic oxidative degradation, which was also observed for oxidation of thiol by Mn oxide and microbial oxidative degradation of OM.[62,63,64]

Selectivity and Oxidative Alterations at the Compound Class Level. To further understand the selectivity and oxidative alterations, we compared the molecular properties of the reacted, persistent, and formed pools for each compound class. The obtained average indices for the three pools of each compound class are provided in Tables S2 and S3, and the number distributions in Figures S4−S7 except for carbohydrates that had too few compounds to have reliable distributions. For each compound class, the differences among the three pools in molecular properties were similar to those observed among OM_{rctd}, OM_{pers}, and OM_{frmd} as described above, but exceptions exist (Tables S1 and S2). For example, carbohydrates with lower NOSC were more prone to be oxidized (Table S2). The exceptions suggest that molecular indices do not accurately reflect the molecular properties pertinent to oxidation.

Studies based on model compounds show that oxidation of aromatic compounds by Mn oxides can result in partial ring cleavage, removal of substituents (e.g., O, N, and S), and polymerization.[65−69] Consistently, the oxidation substantially decreased AI_{mod} of PAH (Table S2). However, the AI_{mod} of polyphenols was changed little by oxidation probably because oxidation of other compound classes produced some new polyphenol compounds, such as via combined ring cleavage, polymerization, and substitution, counterbalancing the reduction of AI_{mod} of polyphenols due to its oxidation. Likewise, many newly produced HuPh compounds at pH 6 (Table 1) probably contributed to the slightly increased AI_{mod} after oxidation (Table 2). The decreased O and N contents (except for Polyph) of the products from oxidation of PAH, polyphenols, and HuPh (Table S3) suggests removal of O and N substituents, although oxidation does not necessarily remove O and N[70] and can even add O to the compound.[31] However, the net decreases in O contents of the products suggest that the removal was dominant. Our data cannot probe polymerization, for which fluorescence spectroscopy is more suitable.[68] Similar to the three aromatic pools, the decreased O and N contents (except for carbohydrates at pH 4) in aliphatics and carbohydrates (Table S3) suggest removal of R-COOH and R-NH_2 groups. Our analysis cannot probe whether the oxidation condensed carbohydrates and amino acids to form aminosugars through the Maillard reaction.[71,72] While the oxidation enriched S in the oxidation products in most cases (Table 2), S associated with PAH was preferentially removed (Table S3), consistent with that S-containing functional groups bound to aromatic rings can be oxidized by Mn oxides to form sulfate.[31,73]

Environmental Implications. Using a model OM−Mn oxide system, this study shows that only a small portion of SRFA was oxidized by δ-MnO_2, and the oxidation, albeit more selective, shared similar compound selectivity rules to DOM adsorption on polar mineral surfaces. We expect that other redox-active minerals with polar surfaces, such as iron oxides,[74] may demonstrate similar behavior in compound selectivity for adsorption and oxidation. The preferential removal of O- and N-containing functional groups of high complexing reactivity implies that oxidation decreases the reactivity of OM for complexation with metals and mineral surfaces besides the electron-donating capacity. Thus, OM associated with Mn oxide surfaces in the environment[21−25,75] may have lower complexing reactivity than those with nonoxidizing minerals. Our results also help understand what types of compounds in DOM can compete with organic pollutants for oxidation by Mn oxides.[31] In addition, the similarities between the abiotic oxidation of DOM by δ-MnO_2 examined in the present study and microbial oxidative degradation, in terms of thermodynamic controls as indicated by NOSC, sulfurization for OM protection, split of aromatic rings, and so on, suggest that OM oxidation by Mn oxide is analogous to OM oxidative degradation catalyzed by enzymes. Thus, the reacted OM compound pool by Mn oxide oxidation likely has a high microbial degradability as well. Similar to assessing soil labile carbon using permanganate-oxidizable carbon,[76] Mn oxide−oxidizable carbon may be an index for detection and identification of labile dissolved organic carbon. Our findings have implications for understanding OM dynamics, particularly in Mn-rich environments, such as marine and lake sediments. Future studies are warranted to test Mn oxides of different mineral phases and DOM of various sources to further understand this important environmental chemical process.

■ ASSOCIATED CONTENT

Supporting Information

The Supporting Information is available free of charge at https://pubs.acs.org/doi/10.1021/acs.est.1c01283.

Synthesis of δ-MnO_2, measurements of DOM and Mn concentration, effects of NaOH treatment, solid-phase extraction, MS data collection and processing, and average molecular properties of the three pools for each compound class and their distributions (PDF)

■ AUTHOR INFORMATION

Corresponding Author

Mengqiang Zhu − *Department of Ecosystem Science and Management, University of Wyoming, Laramie, Wyoming 82071, United States;* orcid.org/0000-0003-1739-1055; Phone: +1 307-766-5523; Email: mzhu6@uwyo.edu

Authors

Jianchao Zhang − *Department of Ecosystem Science and Management, University of Wyoming, Laramie, Wyoming 82071, United States; School of Earth System Science, Institute of Surface-Earth System Science, Tianjin University, Tianjin 30072, China*

Amy M. McKenna − *National High Magnetic Field Laboratory, Florida State University, Tallahassee, Florida 32310, United States;* orcid.org/0000-0001-7213-521X

Complete contact information is available at: https://pubs.acs.org/10.1021/acs.est.1c01283

Notes

The authors declare no competing financial interest.

https://doi.org/10.1021/acs.est.1c01283
Environ. Sci. Technol. 2021, 55, 7741−7751

FT-ICR MS data is publicly-available via Open Science Framework DOI 10.17605/OSF.IO/A7T5H.

■ ACKNOWLEDGMENTS

This work was supported by the National Science Foundation under DEB-2027284. Part of this work was performed at the National High Magnetic Field Laboratory ICR User Facility, which is supported by the National Science Foundation Division of Chemistry and Division of Materials Research through DMR-1644779 and the State of Florida.

■ REFERENCES

(1) Aiken, G. R.; Hsu-Kim, H.; Ryan, J. N. Influence of dissolved organic matter on the environmental fate of metals, nanoparticles, and colloids. *Environ. Sci. Technol.* **2011**, *45*, 3196−3201.
(2) Baken, S.; Degryse, F.; Verheyen, L.; Merckx, R.; Smolders, E. Metal complexation properties of freshwater dissolved organic matter are explained by its aromaticity and by anthropogenic ligands. *Environ. Sci. Technol.* **2011**, *45*, 2584−2590.
(3) Paller, M. H.; Harmon, S. M.; Knox, A. S.; Kuhne, W. W.; Halverson, N. V. Assessing effects of dissolved organic carbon and water hardness on metal toxicity to Ceriodaphnia dubia using diffusive gradients in thin films (DGT). *Sci. Total Environ.* **2019**, *697*, No. 134107.
(4) Córdova, S. C.; Olk, D. C.; Dietzel, R. N.; Mueller, K. E.; Archontouilis, S. V.; Castellano, M. J. Plant litter quality affects the accumulation rate, composition, and stability of mineral-associated soil organic matter. *Soil Biol. Biochem.* **2018**, *125*, 115−124.
(5) Cotrufo, M. F.; Wallenstein, M. D.; Boot, C. M.; Denef, K.; Paul, E. The Microbial Efficiency-Matrix Stabilization (MEMS) framework integrates plant litter decomposition with soil organic matter stabilization: do labile plant inputs form stable soil organic matter? *Global Change Biol.* **2013**, *19*, 988−995.
(6) Kwan, W. P.; Voelker, B. M. Decomposition of hydrogen peroxide and organic compounds in the presence of dissolved iron and ferrihydrite. *Environ. Sci. Technol.* **2002**, *36*, 1467−1476.
(7) Zhuo, X.; Huang, H.; Lan, F.; He, C.; Pan, Q.; Zhang, Y.; Shi, Q. Molecular transformation of dissolved organic matter in high-temperature hydrogen peroxide oxidation of a refinery wastewater. *Environ. Chem. Lett.* **2019**, *17*, 1117−1123.
(8) Allard, S.; Gutierrez, L.; Fontaine, C.; Croué, J.-P.; Gallard, H. Organic matter interactions with natural manganese oxide and synthetic birnessite. *Sci. Total Environ.* **2017**, *583*, 487−495.
(9) Chorover, J.; Amistadi, M. K. Reaction of forest floor organic matter at goethite, birnessite and smectite surfaces. *Geochim. Cosmochim. Acta* **2001**, *65*, 95−109.
(10) Stuckey, J. W.; Goodwin, C.; Wang, J.; Kaplan, L. A.; Vidal-Esquivel, P.; Beebe, T. P.; Sparks, D. L. Impacts of hydrous manganese oxide on the retention and lability of dissolved organic matter. *Geochem. Trans.* **2018**, *19*, No. 6.
(11) Sunda, W. G.; Kieber, D. J. Oxidation of humic substances by manganese oxides yields low-molecular-weight organic substrates. *Nature* **1994**, *367*, 62−64.
(12) Waite, T. D.; Wrigley, I. C.; Szymczak, R. Photoassisted dissolution of a colloidal manganese oxide in the presence of fulvic acid. *Environ. Sci. Technol.* **1988**, *22*, 778−785.
(13) Wang, Q.; Yang, P.; Zhu, M. Structural transformation of birnessite by fulvic acid under anoxic conditions. *Environ. Sci. Technol.* **2018**, *52*, 1844−1853.
(14) Wang, Q.; Yang, P.; Zhu, M. Effects of metal cations on coupled birnessite structural transformation and natural organic matter adsorption and oxidation. *Geochim. Cosmochim. Acta* **2019**, *250*, 292−310.
(15) Janusz, G.; Kucharzyk, K. H.; Pawlik, A.; Staszczak, M.; Paszczynski, A. J. Fungal laccase, manganese peroxidase and lignin peroxidase: Gene expression and regulation. *Enzyme Microb. Technol.* **2013**, *52*, 1−12.
(16) Whalen, E. D.; Smith, R. G.; Grandy, A. S.; Frey, S. D. Manganese limitation as a mechanism for reduced decomposition in soils under atmospheric nitrogen deposition. *Soil Biol. Biochem.* **2018**, *127*, 252−263.
(17) Laszakovits, J. R.; Somogyi, A.; MacKay, A. A. Chemical alterations of dissolved organic matter by permanganate oxidation. *Environ. Sci. Technol.* **2020**, *54*, 3256−3266.
(18) Wenk, J.; Aeschbacher, M.; Salhi, E.; Canonica, S.; von Gunten, U.; Sander, M. Chemical oxidation of dissolved organic Matter by chlorine dioxide, chlorine, and ozone: effects on its optical and antioxidant properties. *Environ. Sci. Technol.* **2013**, *47*, 11147−11156.
(19) Huang, J.; Zhang, H. Redox reactions of iron and manganese oxides in complex systems. *Front. Environ. Sci. Eng.* **2020**, *14*, No. 76.
(20) Post, J. E. Manganese oxide minerals: crystal structures and economic and environmental significance. *Proc. Natl. Acad. Sci. U.S.A.* **1999**, *96*, 3447−3454.
(21) Sunda, W. G.; Huntsman, S. A.; Harvey, G. R. Photoreduction of manganese oxides in seawater and its geochemical and biological implications. *Nature* **1983**, *301*, 234−236.
(22) Xu, X.; Ding, H.; Li, Y.; Lu, A.; Li, Y.; Wang, C. Mineralogical characteristics of Mn coatings from different weathering environments in China: clues on their formation. *Mineral. Petrol.* **2018**, *112*, 671−683.
(23) Anschutz, P.; Dedieu, K.; Desmazes, F.; Chaillou, G. Speciation, oxidation state, and reactivity of particulate manganese in marine sediments. *Chem. Geol.* **2005**, *218*, 265−279.
(24) Madison, A. S.; Tebo, B. M.; Mucci, A.; Sundby, B.; Luther, G. W. Abundant porewater Mn(III) Is a major component of the sedimentary redox system. *Science* **2013**, *341*, 875−878.
(25) Frierdich, A. J.; Hasenmueller, E. A.; Catalano, J. G. Composition and structure of nanocrystalline Fe and Mn oxide cave deposits: Implications for trace element mobility in karst systems. *Chem. Geol.* **2011**, *284*, 82−96.
(26) Burdige, D. J. The biogeochemistry of manganese and iron reduction in marine sediments. *Earth-Sci. Rev.* **1993**, *35*, 249−284.
(27) Tebo, B. M.; Johnson, H. A.; McCarthy, J. K.; Templeton, A. S. Geomicrobiology of manganese(II) oxidation. *Trends Microbiol.* **2005**, *13*, 421−428.
(28) Ma, D.; Wu, J.; Yang, P.; Zhu, M. Coupled manganese redox cycling and organic carbon degradation on mineral surfaces. *Environ. Sci. Technol.* **2020**, *54*, 8801−8810.
(29) Coward, E. K.; Ohno, T.; Sparks, D. L. Direct evidence for temporal molecularfractionation of dissolved organic matter at the iron oxyhydroxide interface. *Environ. Sci. Technol.* **2019**, *53*, 642−650.
(30) Lv, J.; Zhang, S.; Wang, S.; Luo, L.; Cao, D.; Christie, P. Molecular-scale investigation with ESI-FT-ICR-MS on fractionation of dissolved organic matter induced by adsorption on iron oxyhydroxides. *Environ. Sci. Technol.* **2016**, *50*, 2328−2336.
(31) Remucal, C. K.; Ginder-Vogel, M. A critical review of the reactivity of manganese oxides with organic contaminants. *Environ. Sci.: Processes Impacts* **2014**, *16*, 1247−1266.
(32) Ding, Y.; Shi, Z.; Ye, Q.; Liang, Y.; Liu, M.; Dang, Z.; Wang, Y.; Liu, C. Chemodiversity of soil dissolved organic matter. *Environ. Sci. Technol.* **2020**, *54*, 6174−6184.
(33) Mentges, A.; Feenders, C.; Seibt, M.; Blasius, B.; Dittmar, T. Functional molecular diversity of marine dissolved organic matter Is reduced during degradation. *Front. Mar. Sci.* **2017**, *4*, 194.
(34) Bai, Y.; Subdiaga, E.; Haderlein, S. B.; Knicker, H.; Kappler, A. High-pH and anoxic conditions during soil organic matter extraction increases its electron-exchange capacity and ability to stimulate microbial Fe(III) reduction by electron shuttling. *Biogeosciences* **2020**, *17*, 683−698.
(35) Koch, B. P.; Witt, M.; Engbrodt, R.; Dittmar, T.; Kattner, G. Molecular formulae of marine and terrigenous dissolved organic matter detected by electrospray ionization Fourier transform ion cyclotron resonance mass spectrometry. *Geochim. Cosmochim. Acta* **2005**, *69*, 3299−3308.
(36) Kramer, R. W.; Kujawinski, E. B.; Hatcher, P. G. Identification of black carbon derived structures in a volcanic ash soil humic acid by

fourier transform ion cyclotron resonance mass spectrometry. *Environ. Sci. Technol.* **2004**, *38*, 3387−3395.
(37) Stubbins, A.; Spencer, R. G. M.; Chen, H.; Hatcher, P. G.; Mopper, K.; Hernes, P. J.; Mwamba, V. L.; Mangangu, A. M.; Wabakanghanzi, J. N.; Six, J. Illuminated darkness: molecular signatures of Congo River dissolved organic matter and its photochemical alteration as revealed by ultrahigh precision mass spectrometry. *Limnol. Oceanogr.* **2010**, *55*, 1467−1477.
(38) Tfaily, M. M.; Chu, R. K.; Tolić, N.; Roscioli, K. M.; Anderton, C. R.; Paša-Tolić, L.; Robinson, E. W.; Hess, N. J. Advanced solvent based methods for molecular characterization of soil organic matter by high-resolution mass spectrometry. *Anal. Chem.* **2015**, *87*, 5206−5215.
(39) Dittmar, T.; Koch, B.; Hertkorn, N.; Kattner, G. A simple and efficient method for the solid-phase extraction of dissolved organic matter (SPE-DOM) from seawater. *Limnol. Oceanogr. Methods* **2008**, *6*, 230−235.
(40) Blakney, G. T.; Hendrickson, C. L.; Marshall, A. G. Predator data station: A fast data acquisition system for advanced FT-ICR MS experiments. *Int. J. Mass Spectrom.* **2011**, *306*, 246−252.
(41) Emmett, M. R.; White, F. M.; Hendrickson, C. L.; Shi, S. D. H.; Marshall, A. G. Application of micro-electrospray liquid chromatography techniques to FT-ICR MS to enable high-sensitivity biological analysis. *J. Am. Soc. Mass Spectrom.* **1998**, *9*, 333−340.
(42) Hendrickson, C. L.; Quinn, J. P.; Kaiser, N. K.; Smith, D. F.; Blakney, G. T.; Chen, T.; Marshall, A. G.; Weisbrod, C. R.; Beu, S. C. 21 tesla fourier transform ion cyclotron resonance mass spectrometer: a national resource for ultrahigh resolution mass analysis. *J. Am. Soc. Mass Spectrom.* **2015**, *26*, 1626−1632.
(43) Smith, D. F.; Podgorski, D. C.; Rodgers, R. P.; Blakney, G. T.; Hendrickson, C. L. 21 tesla FT-ICR mass spectrometer for ultrahigh-resolution analysis of complex organic mixtures. *Anal. Chem.* **2018**, *90*, 2041−2047.
(44) Corilo, Y. E. *PetroOrg Software*; Florida State University, Omics LLC: Tallahassee, Fl, 2014.
(45) Kendrick, E. A mass scale based on CH2 = 14.0000 for high resolution mass spectrometry of organic compounds. *Anal. Chem.* **1963**, *35*, 2146−2154.
(46) Savory, J. J.; Kaiser, N. K.; McKenna, A. M.; Xian, F.; Blakney, G. T.; Rodgers, R. P.; Hendrickson, C. L.; Marshall, A. G. Parts-per-billion fourier transform ion cyclotron resonance mass measurement accuracy with a "walking" calibration equation. *Anal. Chem.* **2011**, *83*, 1732−1736.
(47) Koch, B. P.; Dittmar, T. From mass to structure: an aromaticity index for high-resolution mass data of natural organic matter. *Rapid Commun. Mass Spectrom* **2006**, *20*, 926−932.
(48) LaRowe, D. E.; Van Cappellen, P. Degradation of natural organic matter: A thermodynamic analysis. *Geochim. Cosmochim. Acta* **2011**, *75*, 2030−2042.
(49) Riedel, T.; Biester, H.; Dittmar, T. Molecular fractionation of dissolved organic matter with metal salts. *Environ. Sci. Technol.* **2012**, *46*, 4419−4426.
(50) Roth, V.-N.; Lange, M.; Simon, C.; Hertkorn, N.; Bucher, S.; Goodall, T.; Griffiths, R. I.; Mellado-Vázquez, P. G.; Mommer, L.; Oram, N. J.; Weigelt, A.; Dittmar, T.; Gleixner, G. Persistence of dissolved organic matter explained by molecular changes during its passage through soil. *Nat. Geosci.* **2019**, *12*, 755−761.
(51) Helms, J. R.; Stubbins, A.; Ritchie, J. D.; Minor, E. C.; Kieber, D. J.; Mopper, K. Absorption spectral slopes and slope ratios as indicators of molecular weight, source, and photobleaching of chromophoric dissolved organic matter. *Limnol. Oceanogr.* **2008**, *53*, 955−969.
(52) Sharpless, C. M.; Aeschbacher, M.; Page, S. E.; Wenk, J.; Sander, M.; McNeill, K. Photooxidation-induced changes in optical, electrochemical, and photochemical properties of humic substances. *Environ. Sci. Technol.* **2014**, *48*, 2688−2696.
(53) Mostafa, S.; Rosario-Ortiz, F. L. Singlet oxygen formation from wastewater organic matter. *Environ. Sci. Technol.* **2013**, *47*, 8179−8186.
(54) Liu, M.; Ding, Y.; Peng, S.; Lu, Y.; Dang, Z.; Shi, Z. Molecular fractionation of dissolved organic matter on ferrihydrite: effects of dissolved cations. *Environ. Chem.* **2019**, *16*, 137−148.
(55) Thurman, E. M.; Junk, M. N. D. W. *Organic Geochemistry of Natural Waters*; Dordrecht: The Netherlands, 1985.
(56) Lv, J.; Han, R.; Huang, Z.; Luo, L.; Cao, D.; Zhang, S. Relationship between molecular components and reducing capacities of humic substances. *ACS Earth Space Chem.* **2018**, *2*, 330−339.
(57) Daniel Sheng, G.; Xu, C.; Xu, L.; Qiu, Y.; Zhou, H. Abiotic oxidation of 17β-estradiol by soil manganese oxides. *Environ. Pollut.* **2009**, *157*, 2710−2715.
(58) Lu, Z.; Lin, K.; Gan, J. Oxidation of bisphenol F (BPF) by manganese dioxide. *Environ. Pollut.* **2011**, *159*, 2546−2551.
(59) Stone, A. T.; Morgan, J. J. Reduction and dissolution of manganese(III) and manganese(IV) oxides by organics: 2. Survey of the reactivity of organics. *Environ. Sci. Technol.* **1984**, *18*, 617−624.
(60) Boye, K.; Noël, V.; Tfaily, M. M.; Bone, S. E.; Williams, K. H.; Bargar, J. R.; Fendorf, S. Thermodynamically controlled preservation of organic carbon in floodplains. *Nat. Geosci.* **2017**, *10*, 415−419.
(61) Subdiaga, E.; Orsetti, S.; Haderlein, S. B. Effects of sorption on redox properties of natural organic matter. *Environ. Sci. Technol.* **2019**, *53*, 14319−14328.
(62) Grice, K.; Schouten, S.; Blokker, P.; Derenne, S.; Largeau, C.; Nissenbaum, A.; Damsté, J. S. S. Structural and isotopic analysis of kerogens in sediments rich in free sulfurised Botryococcus braunii biomarkers. *Org. Geochem.* **2003**, *34*, 471−482.
(63) Sinninghe Damste, J. S.; De Leeuw, J. W. Analysis, structure and geochemical significance of organically-bound sulphur in the geosphere: State of the art and future research. *Org. Geochem.* **1990**, *16*, 1077−1101.
(64) Eitel, E. M.; Zhao, S.; Tang, Y.; Taillefert, M. Effect of manganese oxide aging and structure transformation on the kinetics of thiol oxidation. *Environ. Sci. Technol.* **2018**, *52* (22), 13202−13211.
(65) Dec, J.; Haider, K.; Bollag, J.-M. Release of substituents from phenolic compounds during oxidative coupling reactions. *Chemosphere* **2003**, *52*, 549−556.
(66) Majcher, E. H.; Chorover, J.; Bollag, J.-M.; Huang, P. M. Evolution of CO_2 during birnessite-induced oxidation of 14C-labeled catechol. *Soil Sci. Soc. Am. J.* **2000**, *64*, 157−163.
(67) Shaikh, N.; Taujale, S.; Zhang, H.; Artyushkova, K.; Ali, A.-M. S.; Cerrato, J. M. Spectroscopic investigation of interfacial interaction of manganese oxide with triclosan, aniline, and phenol. *Environ. Sci. Technol.* **2016**, *50*, 10978−10987.
(68) Wu, P.; Fu, Q.-L.; Zhu, X.-D.; Liu, C.; Dang, F.; Müller, K.; Fujii, M.; Zhou, D.-M.; Wang, H.-L.; Wang, Y.-J. Contrasting impacts of pH on the abiotic transformation of hydrochar-derived dissolved organic matter mediated by δ-MnO2. *Geoderma* **2020**, *378*, No. 114627.
(69) Zhang, H.; Huang, C.-H. Oxidative Transformation of Fluoroquinolone Antibacterial Agents and Structurally Related Amines by Manganese Oxide. *Environ. Sci. Technol.* **2005**, *39*, 4474−4483.
(70) Stone, A. T.; Morgan, J. J. Reduction and dissolution of manganese(III) and manganese(IV) oxides by organics. 1. Reaction with hydroquinone. *Environ. Sci. Technol.* **1984**, *18*, 450−456.
(71) Jokic, A.; Frenkel, A. I.; Vairavamurthy, M. A.; Huang, P. M. Birnessite catalysis of the Maillard reaction: Its significance in natural humification. *Geophys. Res. Lett.* **2001**, *28*, 3899−3902.
(72) Zou, J.; Huang, J.; Yue, D.; Zhang, H. Roles of oxygen and Mn (IV) oxide in abiotic formation of humic substances by oxidative polymerization of polyphenol and amino acid. *Chem. Eng. J.* **2020**, *393*, No. 124734.
(73) Dong, J.; Li, Y.; Zhang, L.; Liu, C.; Zhuang, L.; Sun, L.; Zhou, J. The oxidative degradation of sulfadiazine at the interface of α-MnO2 and water. *J. Chem. Technol. Biotechnol.* **2009**, *84*, 1848−1853.
(74) Bauer, I.; Kappler, A. Rates and extent of reduction of Fe(III) compounds and O_2 by humic substances. *Environ. Sci. Technol.* **2009**, *43*, 4902−4908.
(75) Johnson, K.; Purvis, G.; Lopez-Capel, E.; Peacock, C.; Gray, N.; Wagner, T.; März, C.; Bowen, L.; Ojeda, J.; Finlay, N.; Robertson, S.; Worrall, F.; Greenwell, C. Towards a mechanistic understanding of carbon stabilization in manganese oxides. *Nat. Commun.* **2015**, *6*, No. 7628.

https://doi.org/10.1021/acs.est.1c01283
Environ. Sci. Technol. 2021, 55, 7741−7751

(76) Tirol-Padre, A.; Ladha, J. K. Assessing the reliability of permanganate-oxidizable carbon as an index of soil labile carbon. *Soil Sci. Soc. Am. J.* **2004**, *68*, 969−978.

https://doi.org/10.1021/acs.est.1c01283
Environ. Sci. Technol. 2021, 55, 7741−7751